Research Square

Preprints are preliminary reports that have not undergone peer review.
They should not be considered conclusive, used to inform clinical practice,
or referenced by the media as validated information.

Spatially Resolved Quantification of the Molecular Functionalization Process using Marker Molecules for Device Applications

Christian Corcoran
Munster Technological University
Liam O'Faolain
Munster Technological University
Nikolay Petkov
Nikolay.petkov@mtu.ie
Munster Technological University

Article

Keywords: EDX, marker molecules, silanization, device substrates, calibrated quantification, spatial resolution

Posted Date: November 13th, 2026

DOI: https://doi.org/10.21203/rs.3.rs-11459842/v1

License: This work is licensed under a Creative Commons Attribution 4.0 International License.
Read Full License

Additional Declarations: No competing interests reported.

Spatially Resolved Quantification of the Molecular Functionalization Process using Marker Molecules for Device Applications

Christian Corcoran[1,2], Liam O'Faolain[1,2], Nikolay Petkov[1,2*]

[1]Munster Technological University, Cork Campus, Rosa Avenue, Bishopstown, Cork, Ireland

[2]Tyndall National Institute, Lee Matings, Cork, Ireland

[*]corresponding author, Nikolay.petkov@mtu.ie

Abstract

Quantifying molecular functionalization efficiency helps predict key properties such as stability, solubility, surface reactivity and morphology, and the electrical or optical performance of devices. In device engineering, functionalization success is usually judged only at final electrical, electrochemical or optical testing. Earlier indications can come from surface-sensitive techniques such as XPS and AFM, or from contact angle measurements, which while well-established cannot provide calibrated chemical quantification with high spatial resolution. Direct, fast and robust quantification immediately after modification with high spatial resolution is therefore desirable, particularly in multi-step fabrication where functionalization is critical to device function, as in molecular sensors. Here we demonstrate a simple, robust method that requires no sample preparation, using conventional energy-dispersive X-ray (EDX) spectroscopy in a scanning electron microscope (SEM). Sulphur-containing silanes bound to silanol groups on silicon oxide function as EDX markers. By combining this with a detailed treatment of electron beam–substrate interaction at varying incident energies, we obtain calibrated, quantitative data on the functionalization. We also examine the limits of EDX quantification and apply it to map functionalization heterogeneity across the substrate, with numerical estimates of the mapping spatial resolution.

Keywords: EDX; marker molecules, silanization; device substrates; calibrated quantification; spatial resolution

Introduction

Surface molecular functionalization is commonly performed to modify the electrical, physical and chemical properties of substrate materials for a diverse range of on-chip applications ranging from immobilization of biorecognition elements which provide molecular selectivity in optical and electronic biosensors[1], to molecular-monolayer control of semiconductor interfacial energetics and charge transport in electronic and optoelectronic devices[2]. Silanization uses covalent reactions of alkyl silanes and the accessible -OH groups, forming siloxane (Si-O-Si) bonds if silicon oxide is the top surface[3]. The popularity of this approach originates mainly from the broad applicability to various oxide surfaces and the multitude of commercially available silanes. While the gold molecular monolayer formation is better understood[4], the reactions at the silicon oxide surface are, however, more complex due to the varying nature, reactivity and localization of the binding silanol groups. Therefore, a careful control of all relevant reaction parameters is mandatory, specifically, when side reactions such as multilayer formation and bulk silane polymerization are also considered. However, it is still a challenge to predict and experimentally quantify the amount of surface molecular functionalities and respectively the functionalization efficiency for silane modified surfaces. Direct and quantifiable data comes mostly from techniques such as thermogravimetric, mass-spectroscopy and XRF complimented by solid state NMR and XPS, that are, however, applied predominantly to powder materials such as silica micro/nanoparticles. Samples such as for example micro-nanofabricated bio-chemical sensors, require fast and reliable quantification in the areas of interest i.e. spatially resolved quantification across the chip surface. Techniques such as secondary ion mass-spectroscopy (SIMS) with its unquestionably high sensitivity (<ppm) and depth resolution, or XPS that can provide additional information about the element chemical environment have, however, limited capability for analysis at different areas across the surface. Spatially resolved and quantifiable maps of the sample molecular structure and composition can be obtained by spectral imaging, mainly employed by using fluorescence, Raman[5,6], or XRF [7] spectral imaging. Extension of these techniques such as for example X-ray photoemission electron microscopy (XPEEM), tip-enhanced Raman or nanoscale IR techniques can provide local spectroscopic information down to nanometres but have no quantification protocols developed yet. Nano-SIMS[8] or atom probe microscopy (APM)[9] can provide chemical information with high sensitivity and high spatial resolution, but with a major common drawback i.e. require highly specialized and expensive equipment, and most importantly, dedicated sample preparation that can introduce unpredictable artefacts.

Spectral imaging using SEM in combination with energy dispersive X-ray (EDX) analysis can provide elemental distribution maps of the sample surface. On a scanning transmission electron microscope (STEM) it has been advanced to the level where identification of individual atomic columns is possible when applied through specialized detectors, thin specimen and techniques that improve signal collection for low probe currents[10]. Although the method has the ultimate atomic resolution, it requires dedicated and destructive sample preparation, with localized elemental mapping only. Moreover, the detection of trace elements at <0.5 at. % (commonly referred as the limit of detection in SEM-EDX)[11] and/or low atomic number (the backbone of molecular functionalities is mostly C-based) has not yet been demonstrated.

The use of marker molecules for quantification has been extensively used in confocal fluorescence biochemical imaging[12]. In analogy to this approach and for the first time, we developed a molecular quantification method by using alkane-thiol marker molecules, attached to the oxide surfaces by silane coupling and analysed by top-down EDX. The quantification method is simple to execute, with no sample preparation and uses self-calibrated quantification with a spatial resolution on a sub-micron level. The distinctiveness of our approach is in

understanding the electron beam-sample surface interactions at different incident excitation energies and linking that knowledge to the thickness of the functionalized layers. The method uses calculated maximum functionalization efficiency based on available surface functionalization sites, compared to simulated and experimental EDX spectra to determine the S/Si at % values. This is a practical and versatile solution for fast and reliable quality control of the molecular functionalization process because i) a variety of alkane thiols molecules are readily available, ii) the detections require minimal sample preparation, and iii) multiple determinations can be programmed to test largely spaced areas on wafer. The quantification methodology can be extended to analysis beyond functionalized oxide surfaces. Specifically, -SH-containing alkanes can be used in Ge passivation and molecular layer doping[13] or in rendering the Au surfaces biocompatible[14].

Methods & Instrumentation

Materials

Hexadecyltrimethylammonium bromide (99%) (CTAB), tetraethyl orthosilicate (98% reagent grade) (TEOS), Hydrochloric acid (37%) (HCl) and Toluene (99.8% anhydrous) were purchased from Sigma Aldrich. 3-mercaptoproypltrimethoxysilane (MPTS) (95%) was purchased from Fisher Scientific. 11-mercaptoundecyltrimethoxysilane (MUTS) was purchased from Alfa Chemistry. Si wafers (DSP, 100, Undoped) were acquired from University Wafers. Ethanol (absolute) was acquired from University Collage Cork. All chemicals were used without further purification.

Preparation of nanoporous silica layers

In a 125mL Nalgene bottle 2.08 g TEOS is mixed with 3 g 0.2 M HCl, 1.8 g H2O and 5 mL EtOH and heated at 60ºC for 1h in a drying oven. The bottle is well sealed to prevent solvent leakage and left to cool down. 0.546 g CTAB is dissolved in 25 ml EtOH and added to the solution forming a coating solution. The mixture is left to sit for 1h before use and consumed within one week. For a single coated layer, the coating solution is spin coated at 2000 rpm on an acetone/IPA cleaned Si chip, cured on a hotplate at 150ºC for 2min. Layers with increasing thickness are obtained by repeating the spin coating step on cured layers. All substrates are calcined at 400 ºC in a tube furnace in air for 4h. A low temperature ramp of 100ºC/h is used to gently remove the nanoporous structure directing agent (CTAB) while minimizing pore collapse. When complete the substrates are left to cool down in the furnace overnight and are further used for silane molecular functionalization.

Silane molecular functionalization

The surface modification is adapted from the Sypabekova et al review on deposition methods[15]. The functionalization is performed under N_2 in a clean, dry Schlenk line to prevent early hydrolysation of the silane and thus non-uniform deposition. Sample pre-treatment is vital to ensure the removal of organics from Si chips and to activate the hydroxyl groups at the surface.

The functionalization process on the native Si oxide substrates starts with a surface clean in a piranha solution for 20 minutes, rinse with DI water and drying at 110ºC for 20 minutes. A Teflon sample holder is added to a three neck round bottom flask, along with the clean, dry Si chips. A vacuum is applied to the flask for 30 minutes using a rotary pump and subsequently flushed with N_2 for the duration of the functionalization. 50mL of anhydrous toluene is added to the flask via syringe and followed by 0.2mL of 3-mercaptoproypltrimethoxy silane. The solution is heated to reflux and reacted for 1h. After cooling, the samples are removed, washed

twice with toluene and baked at 110°C for 15min. The same functionalization process is used for the molecular functionalization of the samples with the nanoporous silica layers.

Energy dispersive X-ray (EDX) spectroscopy

For the top-down EDX analysis, the samples were loaded to a dual-beam FEI Helios Nanolab 600i SEM equipped with an Oxford Instruments X-MAX 80 detector. The measurements were performed in a point-and-ID mode, by using either at 3 or 5kV incident excitation beams until one million counts where collected. For each sample at least 5 parallel measurements were taken at locations across the sample surface separated by about 5 μm in a total area of about 100 μm^2. For the analysis of milled areas focussed ion-beam milling (FIB) was performed at 30kV with corresponding currents to control the milled depth of the nanoporous layers. The EDX analysis of the milled nanoporous layers was performed in either a point-and-ID mode or in elemental mapping mode. The quantification of the EDX spectra was performed by calibrating against library standards embedded in the Oxford Instruments EDX acquisition software. The S/Si at % values for multiple parallel measurements obtained for each sample were statistically evaluated to calculate averaged values and standard deviation (SD) values (see Table 1 in SI). All functionalized samples were imaged by top-down SEM at 3 or 5kV, and analysed for surface roughness by atom force microscopy (AFM, Horiba LabRAM Nano) Cross-sectional TEM lamella samples were obtained by common FIB milling techniques, using the dual-beam FEI Helios Nanolab system. The scanning transmission electron microscopy (STEM) equipped with an EDX detector was used to obtain x-sectional analysis of the lamella samples, and to obtain x-sectional S/Si at. % data. The analysis was performed in a line-scan and mapping mode, the corresponding average S/Si at. % vales obtained by pixel-by-pixel data analysis from a line-scan or a map.

Numerical calculations

To calculate the theoretical maximum S/Si at. % detectable by EDX, a geometric model was constructed to estimate the number of Si and S atoms within the X-ray interaction. The native Si oxide was considered non-porous i.e. no accessible -OH groups within the volume of the layer but only at its open top surface, while nanoporous layers have accessible inner-layer surface area covered with reactive silanols. The interaction volumes for top-down EDX acquisition were approximated as cylindrical volumes: for 5 kV, radius r = 200 nm and depth h = 250 nm ($V_{int} \approx 1.57 \times 10^9$ nm³), and for 3 kV, r = 30 nm and h = 80 nm ($V_{int} \approx 1.13 \times 10^7$ nm³), based on McGill group Monte Carlo e-beam/substrate interactions for SiO_2/Si stack. The number of Si atoms in the corresponding V_{int} the Si substrate were estimated by the number of atoms in a Si unit cell, while the atoms contributed by the SiO_2 matrix was derived from the bulk density of amorphous silica (ρ = 2.2 g cm^{-3}), scaled down by the solid fraction (1 − porosity) with 22% porosity, measured by ellipsometry for the nanoporous layers deposited. The number of Si and S atoms from the silane i.e. the number of grafted silane molecules was estimated from the available surface area within the interaction volume, parameterised as a specific surface (SA) ranging from 0.1 to 1.0 nm² nm^{-3}, and an assumed surface silanol density of either 3 or 5 Si–OH nm^{-2}. These silanol density bounds follow values reported for hydroxylated amorphous silica in the literature[4,17]. As discussed in the Results Section, the S/Si at. % values predicted by the geometrical calculations are governed by the fraction of the corresponding layers i.e. i) the Si substrate, ii) silica (nonporous or nanoporous) and silane molecules attached to 3 or 5 Si–OH nm^{-2} groups from the oxide in the corresponding interaction volumes generating X-rays (Figure 1b and 3b).

To benchmark these calculations, we preformed parallel estimations employing Oxford Instrument's proprietary LayerProbe® algorithms to simulate top-down EDX spectra and

calculate the S/Si at. % values based on the embedded quantification procedure in the EDX acquisition software (Aztec®) using library of standards. The LayerProbe® simulation models use Si as substrate and we add silica and sulphur layers with thickness of 2.5 and 1 nm, correspondingly, for the native oxide simulations. While the density of the amorphous SiO_2 (ρ = 2.2 g cm^{-3}) is constant the density of the S-containing functionalization layer was introduced as a variable, starting at 0.1 g/cm^3 which approximates about two silane molecules (respectively coupling -OH groups) per nm^2. The nanoporous layers were simulated by having the Si substrate covered by a composite layer with an overall stoichiometry, that is taken directly from a x-sectional STEM EDX analysis of a thick functionalized nanoporous silica layer. The quantified S/Si at. % values from the x-sectional analysis suggested uniform overall stoichiometry of about $S_{0.025}Si_{0.33}O_{0.635}$ which was introduced in the model for layers with different thickens and density of 80% of the amorphous silica density to accommodate for the porosity of the layers.

Results and Discussion

The simplest approach for Si substrate functionalization is by reacting alkyl silanes to the accessible silanol (Si-OH) groups at the native Si oxide. As shown in Figure 1a), the probe molecule we used is a mercapto-alkyl silane with a thiol (-SH) end group that allows for silane spectral identification and determination based on the sulphur EDX signals. Specifically, the sulphur has a relatively simple X-ray characteristic spectrum with K_α signals generated at 2.32 kV allowing for using incident excitation e-beams with energy as low as 3 kV. Unlike, commonly used >10kV excitation beams, with such a low incident energy, the X-ray generation volume is much closer to the substrate surface leading to minimized contribution of the substrate. Figure 1a) schematically outlines this effect demonstrating the difference in the e-beam interaction volumes when 3 and 5 kV beams are directed at the Si surface covered with a 2.5 nm native oxide (Figure 1c). The characteristic X-rays are generated within the interaction volume, spreading laterally and within the depth of the substrate. The dimensions of the interaction volumes (V_{int}) are obtained by Monte Carlo e-beam/substrate simulations using win-Xray simulator[16] and were used to calculate the S/Si at. %. The details of this purely geometrical approach are given in the Methods Section, with the main parameters used outlined in Figure 1 b. Qualitatively, due to the smaller V_{int} depth at 3kV, the overall Si fraction (f_{Si}) in the V_{int} is reduced, that translates directly into higher contribution of the surface layer containing the silanes with -SH groups. Quantitatively, this is seen in the calculated S/Si at. %, shown Figure 2 a), whereby an increase by an order of magnitude is predicted when 3 kV incident beams are used instead of 5 kV. Remarkably, the expected increase in the S/Si at. % from the higher number of -OH groups available for silane coupling is only about 50% (Figure 2a), which is much lower than the projected increase by using lower excitation energy beams for analysis.

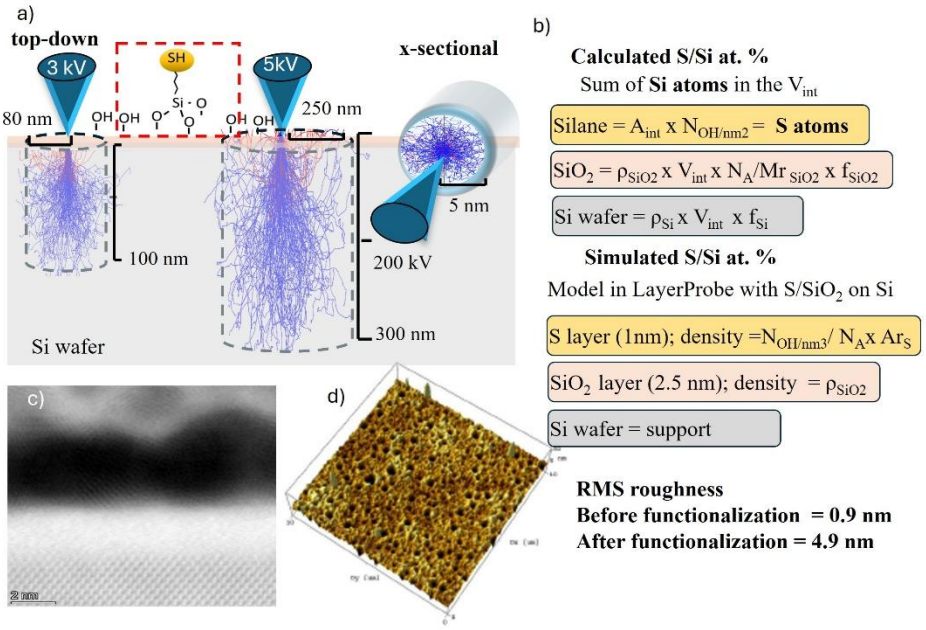


Figure 1: a) Schematics of the e-beam/substrate interactions generating characteristic X-rays during top-down (3 and 5 kV) and x-sectional EDX for native oxide surface on Si, b) main parameters used for calculated and LayerPrbe® simulated S/Si at. % for top-down (3 and 5 kV). c) x-sectional STEM image of the functionalized native Si oxide and d) corresponding 3D AFM map of the surface roughness.

In Figure 1 a), we also schematically compare the top-down *vs* x-sectional X-ray generation volumes and the corresponding benefits in obtaining higher S/Si at. % values. When preforming EDX on a STEM with a 200 kV e-beam, the whole lamella thickness (approximately 100 nm) is within the interaction volume, while the spread of the interactions is minimal, encompassing both the native oxide, carrying the -SH functionalities and the Si substrate However, even for such a thin S-baring oxide, its fraction within the x-sectional interaction volume is much larger and exceeds by far its contribution in comparison to the top-down measurement geometry. Once more, this is demonstrated quantitatively in Figure 2 a) i.e., the calculated x-sectional S/Si at. % values are about an order of magnitude higher than the top-down 3kV, and two orders than the 5 kV detections.

We further validate the S/Si at. % values calculated by using the LayerProbe® algorithm integrated in the Oxford Instrument's proprietary software. The LayerProbe® simulation model uses S-containing and SiO_2 layers on Si (see Methods Section) to obtain simulated spectra and find the S/Si at. % values by the embedded digital library of standards. As seen in Figure 2a), dotted lines, the simulated S/Si at. % values show consistently higher values then the ones calculated by the geometrical approach, and most importantly confirm favourably the main finding i.e. the use of lower (3kV) incident e-beam will provide higher, by an order of magnitude, S/Si at. % determinations. The simulated values increase steadily with the number of the -OH groups at 3 kV as expected, however at 5 kV the values do not show any trend and vary only marginally. In fact, the S-signals in the 5 kV simulated spectra were not quantifiable when calibrating against the embedded digital library standards.

To this end, in Figure 2 a), we compare the numerical predictions with our experimental results (red dots). Example spectrum plots for the 3 and 5 kV top-down, as well as x-sectional STEM EDX measurements are shown Figure 2 b). Clearly, the x-sectional data shows a well-defined S-signal at around 2.32 kV, while the top-down measurements at 5 kV showed only a base-line signal around the S characteristic line. In comparison the top-down 3 kV spectra indicated a

weak S-signal above the noise. We note, that for the quantification purposes the top-down EDX spectra were collected at 5 locations, separated by minimum of 5µm in a total area of above 100 µm^2 as demonstrated in Figure 2c), while the x-sectional analysis was done as spectral maps and lines scans, where each pixel carries spectral information (Figure 2 d-e). In agreement with the baseline S-signal seen for the top-down 5kV measurements, the quantification produced no meaningful S/Si at. % results, with values below 0.01 at %. The S/Si at. % determined from the top-down 3 kV measurements, however, showed values that are higher than the range of values obtained by both the geometrical calculations and LayerProbe® simulations.

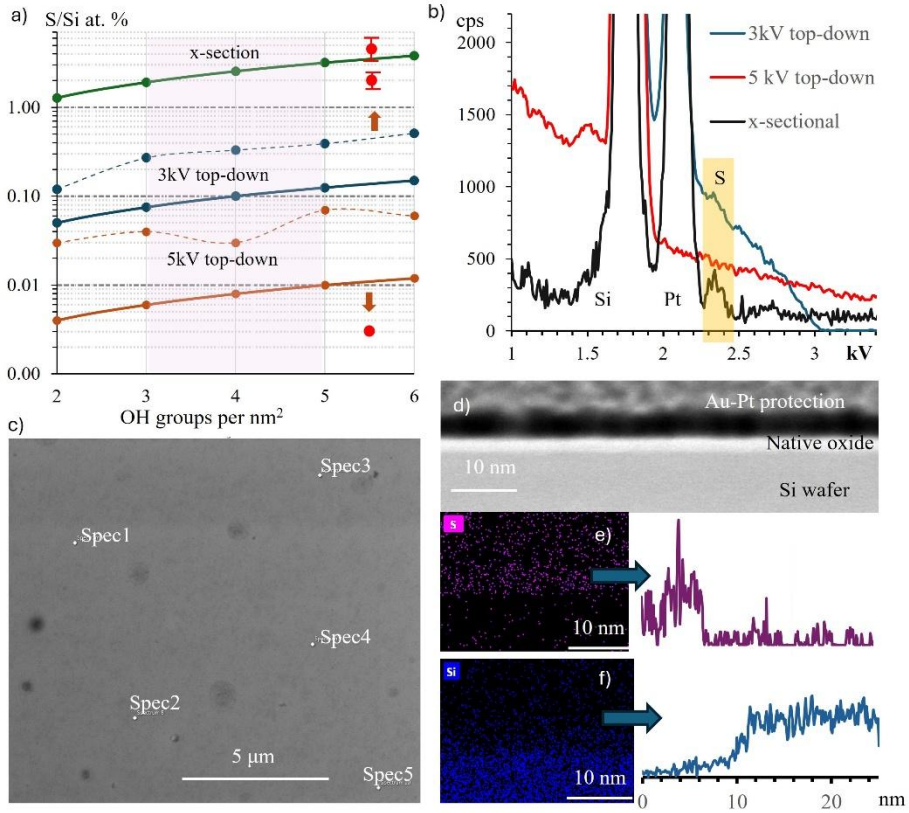


Figure 2: a) Calculated (solid lines) and simulated (doted lines) S/Si at. % values for top-down and x-sectional measurements with corresponding experimentally determined values in red from a functionalized native oxide sample, b) EDX spectral plots used to determine the values in a), c) SEM image of the top surface depicting locations of spectra obtained for the 3kV top-down measurements and d) x-sectional STEM image, e) and f) corresponding S and Si EDX elemental maps. The S and Si signal profiles across the native oxide layer are also shown.

By comparison, the x-sectional experimental data collaborated well with the predicted S/Si at. %, with an average value slightly above predicted for the largest number of -OH groups available for coupling. While we have no estimate of the actual number of the -OH groups on the native oxide, the range of values reported are 3 to 5 -OH groups per nm^2 for various types of silicas[17], indicated with a pink band in Figure 2a). The results from the 3kV and x-sectional determinations suggest higher S/Si at. % values for this range of -OH groups when compared to the predicted ones. One can explain this overestimation by looking at the main assumption i.e., in the predictions we assume that the silane molecules can react with a silanol group from the oxide surface only. We cannot exclude possible silane-to-silane cross-coupling that can increase the S content on the surface. The AFM images taken (Figure 1 d) of the native oxide

surface after silane treatment support that claim. There is almost five times increase in the root-mean-square (RMS) roughness for the silane modified surface in comparison to the piranha cleaned native oxide Si surface before functionalization. This supports the claim that the silane coupling is not fully limited to the silanol groups but also parallel reaction with other silane molecules forming larger aggregates at the surface is possible.

The development of a calibrated determination of the molecular functionalization process utilizing top-down EDX analysis, however, was not possible with the native oxide samples. Therefore, thicker silica layers with varying thickness and internal surface area baring higher number of -OH groups were deposited and reacted with the -SH containing marker molecules, schematically shown in Figure 3 a). As with native oxide, we assumed single molecule attachment per available -OH group and uniform functionalization efficiency across the total thickness of the nanoporous layer. Hence nanoporous layers with open and accessible porosity were simulated, experimentally developed and used for the quantification (Figure 3 and 4). Once more, guided by the Monte-Carlo simulations of the e-beam substate interactions, the dimensions of interaction cylinders generating characteristic x-rays were determined and used to calculate the S/Si at. %. With a 5 kV incident beam the predicted depth of interactions was about 350 nm, while the 3 kV resulted in interaction depth of about 100 nm. Hence, a 5 kV incident beam and a relatively large thickness range of the layers (about 50 – 500 nm) were chosen to obtain higher number of experimental S/Si at. % values for the development of the calibrated quantification procedure. We note that one can use a 3kV incident beam, however, in the thickness range above about 100 nm there will be no increase in the S/Si at. % values, limiting the quantification range of the experimental S/Si at. % data points.
We purposely choose ordered nanoporous silica (also known as mesoporous silica) developed by evaporation induced self-assembly (EISA) due to i) its easily controlled thickness of the layers by dilution or repeated spin-coating steps, ii) the available data about surface area and OH groups number density studied mostly for powdered mesoporous silicas but transferable to layers if accessible porosity is present and iii) the well-known use of nanoporous silicas as a support for chemisorption and pre-concentration of the analyte. The nanoporous layers were analysed structurally by electron microscopy verifying accessible porosity and controllable layer thickness as shown in Figure 3 c) and d). Well-ordered pore arrangement with pore openings of about 2-3 nm were found at the surface of the layers, while the layer thickness was controlled by consecutive spin-coating/drying steps before final surfactant removal step to obtain nanoporous layers for functionalization (SI, Figure 1 of different thickness nanoporous layers). As with the native oxide samples, we used x-sectional STEM to quantify the S/Si at. % content. Unlike the native oxide, however, here we have a much thicker oxide layer (Figure 3d), whereby the x-sectional interaction volume is within the oxide layer in its entire thickness as schematically shown in Figure 3 a). The average S/Si at. % of 7.44, with a standard deviation (pixel to pixel in the spectral line-scan) of 0.035 at. % across the layer thickness was determined (Figure 3e). The line-scan and the quantified S/Si at. % values suggest uniform overall stoichiometry of about $S_{0.025}Si_{0.33}O_{0.635}$ of the nanoporous layer after the functionalization. We used this stoichiometry when building the model for the LayerProbe® simulations. Figure 3 b) shows the main parameters used for calculating and simulating the S/Si at. % values based on the geometry of the 5kV interaction volume and the LayerProbe® algorithm (additional information given in the Methods Section). Notably, for the geometrical calculations we used experimentally determined porosity by ellipsometry that showed averaged values of about 22 %, however values for the accessible surface area (SA) of the layers were not available. Hence, we introduced the SA as a variable in our calculations, alongside the commonly reported values for the number of the -OH groups/nm^2 – three and five -OH groups.

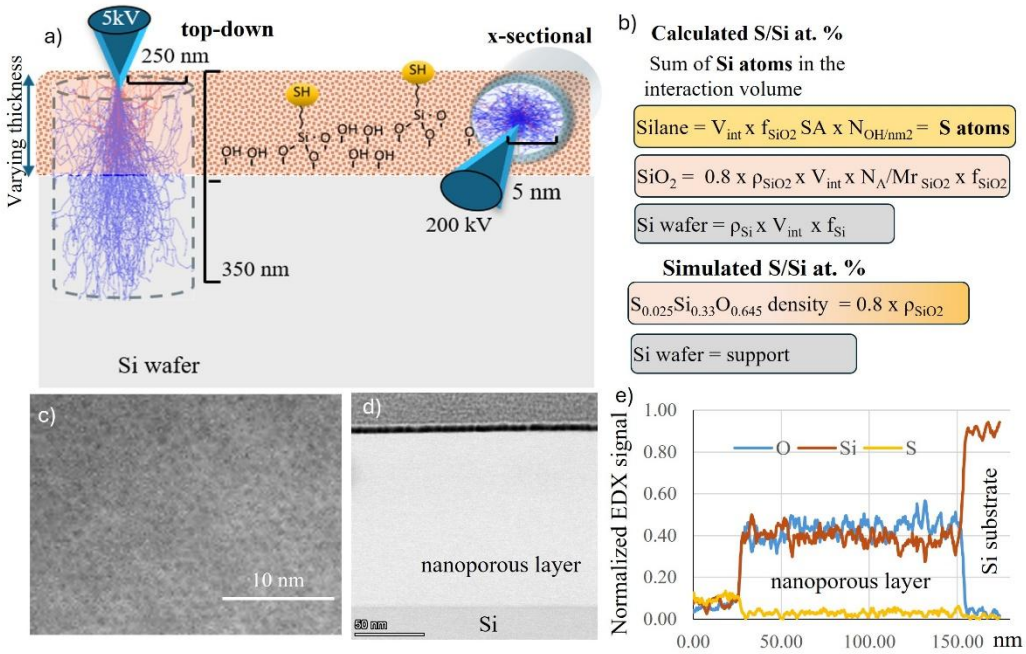


Figure 3: a) Schematics of the e-beam/substrate interactions generating characteristic X-rays during top-down (5 kV) and x-sectional EDX for functionalized nanoporous silica surface on Si, b) main parameters used for calculated and LayerPrbe® simulated S/Si at. % for top-down analysis, c) top-down SEM image and d) x-sectional STEM image of the functionalized nanoporous oxide layer with 120 nm thickness and e) corresponding x-sectional EDX elemental line profiles.

The S/Si at. % values calculated by using the geometry of the interaction volume for relevant thickness levels are shown in Figure 4 a), solid lines. Starting with the lowest practical thickness of the layers of about 30 nm, values in the 0.1 to 1.0 at. % range are predicted. These values are already within the expected detection limit of the EDX technique[18] and further rise as a function of the layers thickness, reaching predicted values of several 10s of S/Si at. % for nanoporous layers with >200 nm thickness. Further confirming these calculations, LayerProbe® simulated values are plotted in Figure 4 a) (dotted lines). The geometrical calculations collaborate very well with the simulations, whereby all simulated values fall within the range predicted by the calculations for a specific surface area of 0.2 nm^2/nm^3. Since, the LayerProbe® simulated data is based on actual x-sectional stoichiometry of the layers (Figure 3a), the grouping of the simulated S/Si at. % values at 0.2 nm^2/nm^3 suggests that the actual internal surface of the nanoporous layers available for functionalization is rather low (see below).

In Figure 4 a) we overlay the experimentally measured S/Si at. % (shown as red dots) for 4 separate functionalized layers produced by repeated spin-coating. For each layer, five spectra were collected separated by at least 5µm (SI Figure 1) and representative EDX spectra are shown in Figure 4b). The spectra shown demonstrate the robustness of our detections and indicate the increase in the S-signal at 2.32 keV with increased thickens of the layers deposited. The average S/Si at. % values quantified from the multiple measured spectra for each layer are shown on a type of calibration plot (Figure 4 b). In fact, we compare two calibration plots of S/Si at. % *vs* layer thickness whereby the thickness is varied by repeated depositions (Figure 4c, red dots) and by using Ga-ion focus-ion beam milling of 5µm wide square areas in a 460 nm film (Figure 4c, red circles). The spectra from each individual square with a corresponding thickness, displayed in SI, Figure 1, follow a steady increase in the S-signal, as well as

appearance of Ga-signal due to the milling process. Most importantly, the S/Si at. % data points from the two calibrations follow linear trendlines with R^2 value of 0.983 for the milled areas and slightly inferior R^2 value of 0.945 for the repeated coatings approach. Note that the slopes of the fitted trendlines are almost equivalent. When the S/Si at. % values from Figure 4 c) are compared to the predicted values in Figure 4 a), it is clearly seen that all experimental values resign in the range of calculated ones for the corresponding layer thickness. They also group around the same SA level of 0.2 nm^2/nm^3 confirming the actual internal specific surface accessible for functionalization.

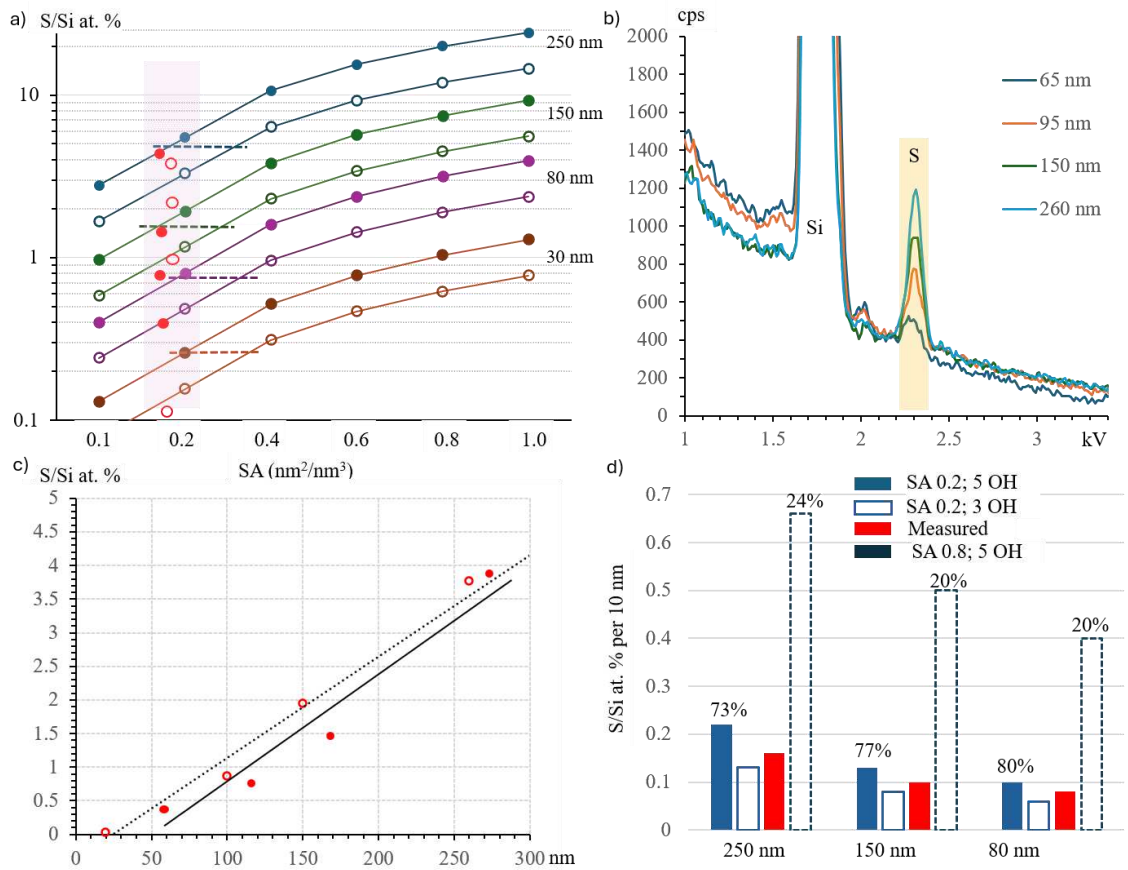


Figure 4: a) Calculated S/Si at. % values (solid lines) as function of the surface area (SA) of the nanoporous silica layers with varying thickness and -OH groups/nm^2: 3 (circles) and 5 (dots). Overlayed on the same plot are the LayerProbe® simulated S/Si at. % (dotted lines) and measured values for layers with thickens shown in b) (red dots) and FIB milled layers (red circles), b) EDX spectral plots for functionalized layers with varying thickness prepared by repeated coating with a marked position of the S-signal, c) Plots of S/Si at. % *vs* nanoporous layer thickness obtained from the spectra in b) (red dots) and FIB milled layers with spectra shown in SI Figure 1, d) Bar charts of the S/Si at. % per 10 nm of the functionalized nanoporous layers with different thickness, comparing predicted (blue) and measured (red) values for corresponding SA (nm^2/nm^3) and number of –OH groups pre nm^2, shown also are the percentage of the maximum predicted S/Si at. % per 10 nm.

In Figure 4 d) we summarize the experimental and calculated S/Si at. % values after normalizing the data to 10 nm of the layer, for varying layer thicknesses. Distinctly, all values scale down with the thickness, outlining once more the thickness effect i.e. higher S/Si at. % values are seen at larger thickness. The experimentally determined values are consistently

higher than the calculated maximum S/Si at. % values for an oxide with SA of 0.2 nm^2/nm^3 and 3 -OH groups pre nm^2. However, for the same SA, the experimental S/Si at. % are about 73 – 80 % of the maximum predicted if we assume that nanoporous oxide is with 5 -OH groups pre nm^2. For such a relatively low SA both results represent upper and lower boundary of the functionalisation efficiency (represented as percentage of the calculated maximum) for the reported range of silanol groups. Arguably, the higher functionalization efficiency for layers with 3 -OH groups pre nm^2 can be understood by taking into consideration possible cross-linking between silane molecules and formation of multilayers as discussed before for the silica native oxide. If 3 -OH groups pre nm^2 are taken but a much higher surface area (0.8 nm^2/nm^3) of the layer is considered, than the functionalization efficiency is reduced drastically to only 20 % of the maximum predicted (Figure 4d). Björk (2024) reported a surface area of 0.88 nm^2/nm^3 for a mesoporous silica films using krypton physisorption at 77 K[19]; the structural similarity of that film to the EISA-derived spin-coated layer used here makes this a relevant reference benchmark for accessible surface area, then the estimated functionalization efficiency is rather low. Other research provides assessment of the nanoporous molecular functionalization efficiency exclusively with methods for powder material analysis such as qNMR[20,21], TGA/CHNSO/FTIR[22] with estimates in the range of 13-46%.

We also provide a useful benchmarking of the quantification methodology developed to non-porous layers that are typically used in device fabrication. Conventional silicon oxide CMOS-compatible coating methods such as physical vapor deposition (PVD) or plasma enhanced chemical vapour deposition (PE-CVD) produce layers with well controlled thickness but with limited internal porosity. Under the main assumption i.e. the S-containing silane molecules attach only at the available -OH groups from the top surface, and do not bond to the internal surface, we calculate the S/Si at. % values for 3 and 5 kV top-down EDX (Figure 5a). The calculations shown are for relatively low thickens levels of about 30 and 80 nm that are typically used during PVD or PE-CVD depositions. Similarly to the thin native oxide, the advantage of using 3kV instead of 5kV is evident, however the thickness effect i.e. higher values are seen at larger thickness, is well seen at 3kV, and only marginally at 5kV. In contrast for the same thickness nanoporous layers with a SA of 0.2 nm^2/nm^3, S/Si at. % values of almost an order of magnitude are predicted (Figure 5a). Even at such relatively low specific surface area, we observe a significant increase in the predicted S/Si at. % values, justifying the use of nanoporous oxides for quantification of the functionalization process. Moreover, the overlayed experimental S/Si at. % values for 3kV measurements (Figure 5a, red dots) agree very well to the predicted and corelate well to the experimental 5kV data shown in Figure 4a) for nanoporous layers with SA of 0.2 nm^2/nm^3 and 3 -OH groups.

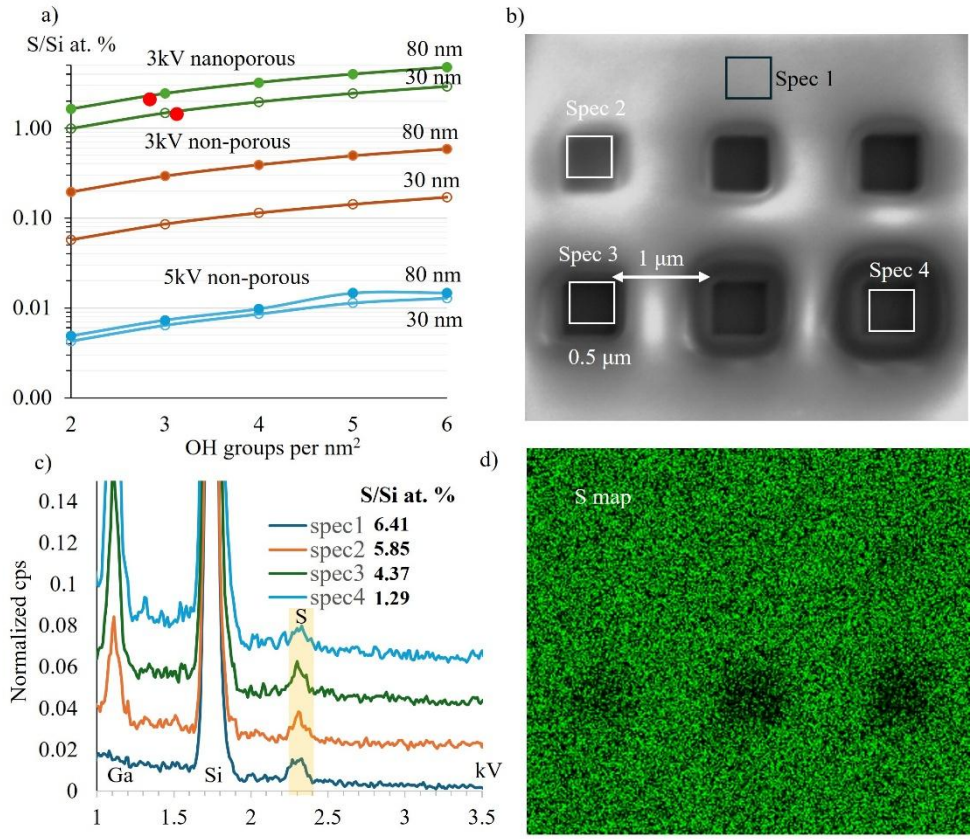


Figure 5: a) Calculated S/Si at. % values for 3 and 5 kV top-down measurements as function of the number of -OH groups pre nm^2 for functionalized silica layers with varying porosity and thickness as depicted in the plots. Overlayed are measured values at 3 kV for with 30 and 80 nm thickens (red dots) b) SEM image and c) EDX sum spectra and d) S-map of a functionalized nanoporous layer with milled areas as described in the text. The S/Si at. % values determined from the areas denoted as spec 1-4 and shown in b) are inserted in c).

We further establish the limits for quantifying the functionalization process in terms of possible heterogeneity across the substrate (spatially resolved quantification). As shown in Figure 3 a), for the top-down geometry at 5 kV, the spread of interactions laterally is with a radius of about 250 nm, which can be taken as the limit in the point-to-point spatial quantification. Practically, however, during the lateral mapping the EDX signals are acquired pixel-by-pixel in the specified area and require relatively high counts number for a reliable quantification. This is of a particular importance when only up to a low at. %, of the quantified element is present at the surface (see the predictions shown in Figure 4a and 5a). To probe these limitations, we used the FIB to mill 0.5µm squares in a thick nanoporous layer with a step of about 50-60 nm per milled square. The structures obtained are shown in Figure 5b), together with the corresponding spectrum plots from selected areas (Figure 5c) obtained at 5kV and the S-EDX map (Figure 5d). Evidently, the squares with lower milled depth (upper row) cannot be distinguish in the S-map from the surrounding unmilled 320 nm functionalized nanoporous layer. However, the spectral plots extracted and the averaged S/Si at. % values (Figure 5 c), showed clear decrease in the S-signal and the corresponding quantified values. It seems that a clear contrast in the S-map between the unmilled and milled areas is only seen, when about 200-220 milled depth is reached (area marked spec3 in the S-map). Looking at the difference between spec1 (no mill) and sepc3, there is about 2 at. % decrease in the S/Si values, giving a value of about 0.1 S/Si at. % per 10 nm of the layer, which agrees well with the values shown in Figure 4d). That once more provides evidence for the robustness of our quantification approach. Moreover, we

establish that the limits for spatially resolved mapping of the S-content, respectively the "patchiness" or the heterogeneity of the molecular functionalization process for features with sub-micron dimensions is at about 2 at. % in the S/Si at content across different areas separated by about 0.5 μm. If we back calculate, based on the volume of the functionalized nanoporous layer that was milled away and the specific surface area of 0.2 nm^2/nm^3 with 3 -OH groups per nm^2, these are about $3x10^7$ molecules attached. If we spread that number of molecules over the top surface of a non-porous layer, forming a monolayer with 3 -OH groups per nm^2, it will cover an area of 10 μm^2. Assuming no contribution of the Si substrate in the EDX detection, for example by performing measurements on a >100 nm thick non-porous oxide, by spectral mapping we should be able to distinguish areas with and without a monolayer that are over 10 μm in size. For a thin (2.5 nm) native silicon oxide, where the contribution of the Si substrate is predominant and the corresponding S/Si at. % values are on order of magnitude lower, the spatially resolved mapping of functionalization heterogeneity within a monolayer would be limited to 100's of μm. Although EDX mapping is routinely used to characterize inorganic materials and comparatively thick coatings, its application to molecular monolayers has remained limited because the elemental signal from a nanometre-scale organic layer is extremely weak relative to the X-ray signal generated within the underlying substrate. Lowering the accelerating voltage reduces the interaction volume and increases surface sensitivity, but it also reduces X-ray generation and restricts the characteristic lines that can be excited, creating an inherent trade-off between sensitivity and spatial resolution.

Conclusions

We have developed molecular quantifications using EDX marker molecules for characterizing functionalized substrate surfaces for device applications. While the method is fast, robust and calibrated, it features several limitations that are thoroughly studied by both numerical calculations and experimental data. Specifically, the top-down EDX quantification of thin native oxide Si surfaces appeared challenging. However, for the first time, we outline numerically the limits for quantification, justifying the use of lower (3kV) energy incident beams, instead of commonly suggested higher energy EDX analysis. In parallel, we showcased the advantage of the x-sectional analysis and support our findings by detailed description of the differences in the x-ray interaction volume by x-sectional and top-down EDX analysis of the functionalized native Si oxide. For the development of calibrated quantification, we extend the method to thicker nanoporous layers, and for the first time established their functionalization efficiency using on top-down EDX as well as spatially resolved mapping of the functionalization heterogeneity across the sample surface. The calibrated quantifications not only followed a robust analytical determination process but also provided critical assessment of the results by comparing to calculated and simulated values. The key to the spatial resolution demonstrated is in using organic molecules with heteroatoms such as sulphur as markers, covalently reacted to the surface. In addition, the methodology is with minimal sample preparation and can be executed on large areas across the substrate by point-and-ID shorter acquisitions or by longer time spectral mapping. The quantification methodology is not limited to analysis of functionalized oxide surfaces. There are -SH-containing alkanes, readily available with different hydrocarbon chains, that can be used in semiconductors passivation or in rendering the Au surfaces biocompatible. Hence, the technique can provide quantifiable information elucidating the successful accomplishment of the substrates modification for a diverse range of molecularly enabled on-chip devices.

Data Availability

All data supporting the findings of this study are available within the paper and its Supplementary Information.

References

1. Morales, M. A. & Halpern, J. M. Guide to selecting a biorecognition element for biosensors. Bioconjug. Chem. 29, 3231–3239 (2018). https://doi.org/10.1021/acs.bioconjchem.8b00592

2. Li, M. et al. Self-assembled monolayers for interfacial engineering in solution-processed thin-film electronic devices: Design, fabrication, and applications. Chem. Rev. 124, 2138–2204 (2024). https://doi.org/10.1021/acs.chemrev.3c00396

3. Smith, E. A. & Chen, W. How to prevent the loss of surface functionality derived from aminosilanes. Langmuir 24, 12405–12409 (2008). https://doi.org/10.1021/la802234x

4. Dietrich, P. M. et al. Quantification of silane molecules on oxidized silicon: Are there options for a traceable and absolute determination? Anal. Chem. 87, 10117–10124 (2015). https://doi.org/10.1021/acs.analchem.5b02846

5. LaLone, V. et al. Quantitative Raman chemical imaging of intracellular drug–membrane aggregates and small-molecule drug precipitates in cytoplasmic organelles. Adv. Drug Deliv. Rev. 202, 115107 (2023). https://doi.org/10.1016/j.addr.2023.115107

6. Li, B., Calvet, A., Casamayou-Boucau, Y., Morris, C. & Ryder, A. G. Low-content quantification in powders using Raman spectroscopy: A facile chemometric approach to sub-0.1% limits of detection. Anal. Chem. 87, 3419–3428 (2015). https://doi.org/10.1021/ac504776m

7. Tsuji, K. et al. New developments of X-ray fluorescence imaging techniques in laboratory. Spectrochim. Acta B At. Spectrosc. 113, 43–53 (2015). https://doi.org/10.1016/j.sab.2015.09.003

8. Chen, Y., Xie, Z., Dong, S., Lei, Q. & Gao, J. High spatial resolution and precision NanoSIMS for sulfur isotope analysis. J. Anal. At. Spectrom. 37, 2529–2536 (2022). https://doi.org/10.1039/D2JA00248E

9. Chae, B.-G. et al. 3D mapping of compositional gradients of core-shell structures in AgInxGa1-xS2 quantum dots by atom probe tomography. Nat. Commun. 17, 4759 (2026). https://doi.org/10.1038/s41467-026-71518-5

10. Wenner, S., Jones, L., Marioara, C. D. & Holmestad, R. Atomic-resolution chemical mapping of ordered precipitates in Al alloys using energy-dispersive X-ray spectroscopy. Micron 96, 103–111 (2017). https://doi.org/10.1016/j.micron.2017.02.007

11. Newbury, D. E. & Ritchie, N. W. M. Performing elemental microanalysis with high accuracy and high precision by scanning electron microscopy/silicon drift detector energy-dispersive X-ray spectrometry (SEM/SDD-EDS). J. Mater. Sci. 50, 493–518 (2015). https://doi.org/10.1007/s10853-014-8685-2

12. Gonçalves, M. S. T. Fluorescent labeling of biomolecules with organic probes. Chem. Rev. 109, 190–212 (2009). https://doi.org/10.1021/cr0783840

13. Gillian Collins, Peter Fleming, Sven Barth, Colm O'Dwyer, John J. Boland, Michael A. Morris, Justin D. Holmes; Alkane and Alkanethiol Passivation of Halogenated Ge Nanowires. *Chem. Mater.* 14 December 2010; 22 (23): 6370–6377. https://doi.org/10.1021/cm1023986

14. Frasconi M, Mazzei F, Ferri T. Protein immobilization at gold-thiol surfaces and potential for biosensing. Anal Bioanal Chem. 2010 Oct;398(4):1545-64. doi: 10.1007/s00216-010-3708-6. Epub 2010 Apr 23. PMID: 20414768.

15. Sypabekova, M. et al. Improvement of the optical cavity-based biosensor's limit of detection using optimal 3-aminopropyltriethoxysilane process. Sci. Rep. 15, 7739 (2025). https://doi.org/10.1038/s41598-025-92151-0

16. Gauvin, R., Lifshin, E., Demers, H., Horny, P. & Campbell, H. Win X-ray: A new Monte Carlo program that computes X-ray spectra obtained with a scanning electron microscope. Microsc. Microanal. 12, 49–64 (2006). https://doi.org/10.1017/S1431927606060089

17. Zhuravlev, L. T. The surface chemistry of amorphous silica: Zhuravlev model. Colloids Surf. A Physicochem. Eng. Asp. 173, 1–38 (2000). https://doi.org/10.1016/S0927-7757(00)00556-2

18. Burgess, S. Determining accurate detection limits for EDS analysis using simulated spectra. Oxford Instruments https://www.oxinst.com/learning/view/article/determining-accurate-detection-limits-for-eds-analysis-using-simulated-spectra (2022).

19. Bjork, E. M. Surface area determination of particle-based mesoporous films using krypton physisorption. ACS Omega 9, 5899–5902 (2024). https://doi.org/10.1021/acsomega.3c07758

20. Kunc, F. et al. Quantification and stability determination of surface amine groups on silica nanoparticles using solution NMR. Anal. Chem. 90, 13322–13330 (2018). https://doi.org/10.1021/acs.analchem.8b02803

21. Cheng, R. et al. Quantitative analysis of porous silicon nanoparticles functionalization by 1H NMR. ACS Biomater. Sci. Eng. 8, 4132–4139 (2022). https://doi.org/10.1021/acsbiomaterials.1c00440

22. Saengdee, L., Pasetto, P. & Sukhawipat, N. Functionalization of mesoporous silica with oligoisoprene brushes: Application as charge for elastomers reinforcement. Prog. Org. Coat. 186, 107988 (2024). https://doi.org/10.1016/j.porgcoat.2023.107988

Acknowledgements

Funding: The authors acknowledge financial support from project funding from Research Ireland project 21/FFPA/10002.

Author Contributions:

Conceptualization, N.P.; methodology, C.C. and N.P.; software, C.C. and N.P.; validation, C.C., N.P. and L.O'F.; formal analysis, C.C. and N.P.; investigation, C.C. and N.P.; resources, N.P.;

data curation, C.C. and N.P.; writing—original draft preparation, C.C.; writing—review and editing, N.P. and L.O'F; visualization, C.C. and N.P.; supervision, N.P. and L.O'F.; project administration, N.P. and L.O'F.; funding acquisition, L.O'F. All authors have read and agreed to the published version of the manuscript.

Competing interests

The author(s) declare no competing interests.

Additional Information

Supplementary Information The online version contains supplementary material available at https://doi.org/doi

Correspondence and requests for materials should be addressed to N.P

Supplementary Files

This is a list of supplementary files associated with this preprint. Click to download.

- 261014QuantificationPaperSupportingInformation.docx